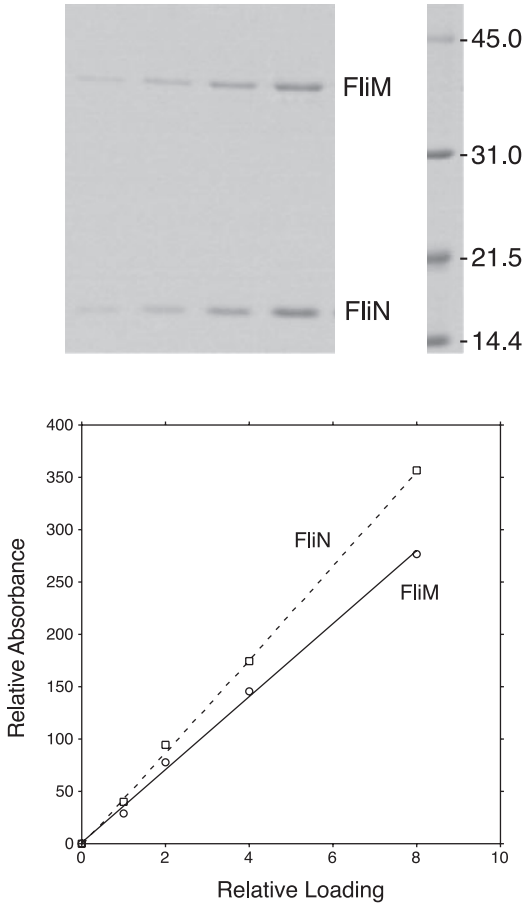

FIG. 8. Quantification of FliM and FliN proteins in the FliM-FliN complex. The gel was stained with Coomassie blue. Relative protein levels were estimated by assuming that the staining intensity of a band is proportional to the mass of protein in the band. The ratio of the slopes of the fitted lines (and thus the ratio of staining intensities for the FliN and FliM bands) is 1.3:1. Given the molecular masses of FliM and FliN (37.2 and 15.1 kDa, respectively), this corresponds to an estimated FliN/FliM ratio of 3.2:1.

tetramer is also supported by the large shape factor (1.4) determined in the velocity-sedimentation experiment. Although the residues at the dimer-dimer interface have dimer-related counterparts that are exposed at the ends of the tetramer, we did not see evidence of any FliN complexes larger than a tetramer. Further end-to-end association of the tetramers might be prevented by the N-terminal parts of the protein, which are sizable (more than 50 residues) but were not sufficiently ordered to be seen in either crystal structure.

The shorter dimensions of the FliN tetramer are 3 to 4 nm, which is comparable to the subunit spacing seen in end views of the C ring (4 nm). The 11-nm dimension of the tetramer is sufficient to span about three-fourths the height of the C ring (19, 31, 68, 79). We therefore propose that the FliN tetramers are arranged in the C ring with their long axes approximately parallel to the axis of the flagellum (Fig. 12). Given such a subunit arrangement, the C ring could be viewed as a fusion of two rings, an upper ring and a lower ring, each formed from a circular array of FliN dimers. Thin-metal replica images of the C rings of *Salmonella* have a two-layer appearance consistent with such an architecture, and partially disrupted C rings sometimes appear to lack portions of the lower layer (32). The C-ring architecture proposed here is probably applicable to a wide range of bacterial species but may not be universal. Certain species (e.g., *Bacillus subtilis*) use the much larger FliY protein in place of FliN (7), and their C rings might be constructed differently.

The present structural study of FliN has some bearing on FliM, because a segment in the C-terminal domain of FliM shows sequence similarity to FliN (46). Several residues are conserved as hydrophobic residues in both proteins, and the structure shows that these residues form much of the core of FliN (Fig. 4; also see Fig. S2 in the supplemental material). The secondary-structure predictions for this part of FliM agree well with the secondary structures seen in the structure of FliN, except that β1 is predicted to be interrupted by a loop in FliM (see Fig. S2 in the supplemental material). Based on the correspondence between the proteins, we propose that the C-terminal domain of FliM is folded like the C-terminal domain of FliN, except that β1 folds back onto itself and β2 and β3 are joined by a reverse turn, which allows the β barrel to be formed from a single chain rather than two chains. This segment of FliM is also the part that binds to FliN (46, 70), and its structural resemblance to FliN may be important for this binding. A similar correspondence has been noted between HrcQB and its binding partner, HrcQA (16).

FliN is essential for flagellar assembly, because deletion of the *fliN* gene results in a nonflagellate phenotype (65). Its functions in assembly are not easily disrupted by point mutations. Irikura et al. (27) analyzed a number of *fliN* mutations and found that flagellar assembly was prevented only by frameshifts or premature termination. Most missense mutations give a *mot* phenotype, in which flagella are assembled but do not rotate. Some rotation was restored when the *mot* mutant proteins were overexpressed, which suggests that the mutations decreased the level of the protein or diminished its ability to form fully functional C rings. The positions of *mot* mutations in the structure appear to be consistent with this suggestion (see Fig. S3 in the supplemental material). One *mot* mutation replaced a fairly well-conserved Gly residue (Gly120 in the *T. maritima* protein) whose ϕ and ψ angles (80° and −10°, respectively) are not as favorable for a larger side chain, one mutation introduced Pro in place of a residue (Leu117) whose ϕ angle (−115°) was incompatible with Pro, and another mutation replaced a fairly well-conserved Pro residue (Pro 78) in the segment that separates α1 from β1. Two *mot* mutations replaced nonpolar residues that are largely buried (positions 92 and 95). The remaining positions that gave a *mot* phenotype (positions 121 and 122) were together on the side surfaces of the tetramer, where they might participate in interactions that stabilize the C ring. One of these mutations (at position 122) was found to cause a reduction in the length of the flagellar hook (43). This might indicate that FliN has a role in binding to hook subunits, as proposed by Makishima and coworkers (43), but it is also consistent with a more general role for FliN in flagellar assembly.

Mutations that affect the CW-CCW bias of the motor (designated *che*, for nonchemotactic) have been reported for five positions in FliN (27). These mutations occur at the hypothesized dimer-dimer interface (residues 99 and 100 in *T. mari-*